Boletim da Sociedade Astronômica Brasileira, **35**, no. 1, 204-205

Relic galaxies and massive compact ETGs from TNG50: local dynamics and global environment

Micheli T. Moura[1], Ana L. Chies-Santos[1], C. Furlanetto[1], & Ling Zhu[2]

[1] Universidade Federal do Rio Grande do Sul – UFRGS, Brasil. e-mail: micheli.moura@ufrgs.br
[2] Shanghai Astronomical Observatory, Chinese Academy of Sciences – SHAO. China.

Abstract. Relic galaxies are massive, compact, and quiescent objects observed in the local Universe that have not experienced any significant interaction episodes or merger events since $z \approx 2$, remaining relatively unaltered since their formation. These galaxies with "frozen" history can provide important clues about the intrinsic processes related to the formation and evolution of massive Early-Type Galaxies (ETGs). Using the high-resolution cosmological simulation TNG50-1 from the Illustris Project, we investigate the assembly history of a sample of massive, compact, old, and quiescent subhalos split by 10% of satellite accretion fraction. We compare the evolutionary pathways at three cosmic epochs: $z = 2$, $z = 1.5$, and $z = 0$, using the orbital decomposition numerical method to investigate the stellar dynamics of each galactic kinematical component and their environmental correlations. Our results point to a steady pathway across time that is not strongly dependent on the mergers or the environment.

Resumo. Galáxias relíquias são objetos massivos, compactos e quiescentes observados no Universo local que não sofreram nenhum episódio de interação significativa ou eventos de fusão desde $z \approx 2$, permanecendo relativamente inalteradas desde sua formação. Essas galáxias com história "congelada" podem fornecer pistas importantes sobre os processos intrínsecos relacionados à formação e evolução de galáxias massivas do tipo Early-type (ETGs). Usando a simulação cosmológica de alta resolução TNG50-1 do Projeto Illustris, investigamos o histórico evolutivo de uma amostra de subhalos massivos, compactos, antigos e quiescentes, separados pela fração de acreção de satélites de 10%. Comparamos os caminhos evolutivos em três épocas: $z = 2$, $z = 1.5$ e $z = 0$, usando o método numérico de decomposição orbital para investigar a dinâmica estelar de cada componente cinemático e suas correlações ambientais. Nossos resultados apontam para um caminho estável ao longo do tempo que não depende muito das fusões ou do ambiente.

Keywords. Galaxies: evolution – Galaxies: structure – Galaxies: kinematics and dynamics

1. Introduction

The difference between massive early-type galaxies (ETGs) and their counterparts at high redshift ($z \gtrsim 2$) is considerable (Trujillo et al. 2007; Buitrago et al. 2008; Belli, Newman, & Ellis 2014). Observations and numerical studies suggest that high-redshift ETGs tend to be compact and smaller in comparison with the local analogs, with half-light radii smaller by a factor of ~ 3 (van der Wel et al. 2014; Naab, Johansson, & Ostriker 2009). A standard scenario for the formation and evolution of ETGs is the two-phase scenario (Trujillo et al. 2007). The initial phase of formation at $z > 2$ is characterized by the rapid growth of the stellar mass by wet mergers leading to a phase with a high star formation rate (SFR), while there is no significant growth of size (e.g., van Dokkum et al. 2015; Zibetti et al. 2020). Due to the quick increase of mass and star formation, one expects that these compact and massive objects quench and become passive. The first stage of formation is the so-called 'red nugget'. The second stage refers to a growth in size surrounding the nugget by dry mergers with other smaller structures. The two-phase scenario associated with the assembly history of ETGs is currently being investigated by observational and numerical approaches (Flores-Freitas et al. 2022; Zhu et al. 2022). Relic galaxies are defined as massive, compact, and quiescent objects observed in the local Universe that have not experienced any significant interaction episodes or important merger events since $z \sim 2$ (the preserved nugget), therefore remaining mainly unaltered since their formation.

2. Methods

To perform the evolutionary dynamical analysis we use the highest resolution cosmological simulation of Illustris Project: TNG50-1[1] (Pillepich et al. 2018), since we are interested in resolving the stellar kinematics of each kinematical component on a galactic scale. We select a sample of 156 massive, compact, quiescent, and old subhalos at $z = 0$, based on the observational literature for mass and size (Belli, Newman, & Ellis 2014) ($M \geq 10^{10}\,\mathrm{M}_\odot$, $R_e \leq 4$ kpc), quiescence (sSFR $< 10^{-11}\,\mathrm{M}_\odot\,\mathrm{yr}^{-1}$), and age ($\geq 5$ Gyr) parameters. To obtain a sample of Relics, we adopt the threshold of 10% for the satellite accretion to separate between Relics and compact ETGs (cETGs). The Relics group is composed of 99 subhalos that have experienced a quiet accretion merging history. The cETGs sample is composed of the remaining 57 subhalos, which even though have experienced mergers, are still compact at $z = 0$. We employ the dynamical decomposition method from Zhu et al. (2022) to investigate the dynamics of each kinematical component (bulge, disk, and hot inner stellar halo) for both samples. This method consists of characterizing the stellar orbits of each component from the phase-space of energy E and angular momentum L_z. In this method, we consider that the stellar particles will have a distribution of the orbital circularity λ_z, thus stellar particles with similar energy and angular momentum remain on similar orbits. The representation of the orbital parameters for each component can be seen in Fig. 1.

3. Results and discussions

We analyze each stellar component distribution in three different redshifts, aiming to trace the evolutionary stellar pathways of cETGs and Relic galaxies. Overall, the total sample composed by cETGs and Relic galaxies share similarities in terms

[1] https://www.illustris-project.org/

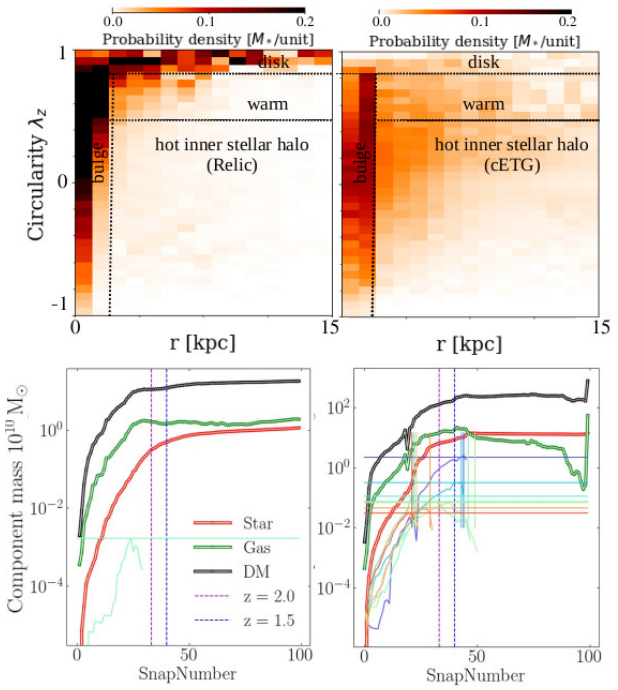

Figure 1. Upper panels: Stellar orbit distribution, $p(r, \lambda_z)$ in the phase-space of circularity (λ_z, r) of two simulated galaxies in TNG50: Relic (left) and a cETG (right) at $z = 0$. The kinematical components are separated by the dashed dark lines. Lower panels: Stellar, gas, and dark matter mass over time of the subhalos in the upper panels in red, green, and black lines, respectively. Dashed lines in magenta and blue indicate z = 2 and z = 1.5. Satellite accretion is illustrated as colored solid lines below the components lines (gas, stars, and DM).

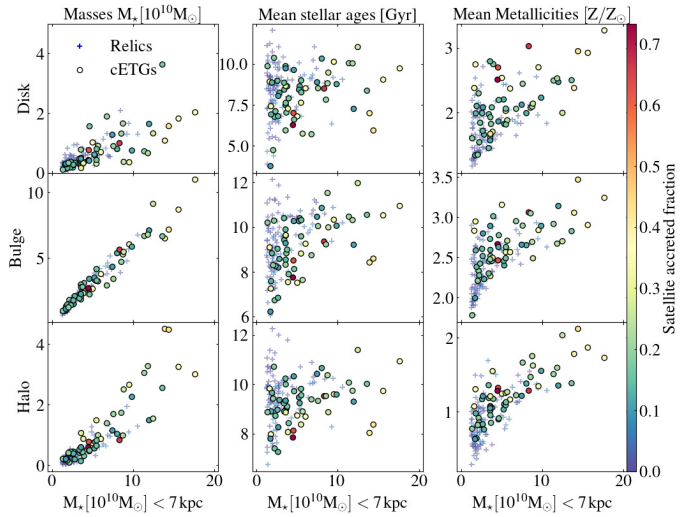

Figure 2. Stellar total mass, mean age, and mean metallicity to each kinematical component at $z = 0$ for Relics and cETGs color-coded by the satellite accretion.

of assembly history, considering general aspects such as age, metallicity, compactness, and environment. At $z = 2$, our sample exhibits similar dynamic characteristics in all kinematic components (bulge, disk, and hot inner stellar halo).

The spread of stellar ages and metallicities among the stellar masses across the components (Fig. 2) illustrates the role of accretion over disk, bulge, and halo. It is expected that some cETGs are outliers in the distribution for higher masses ($M_\star$ within 7 kpc) due to late accretion. Except for these outliers, the

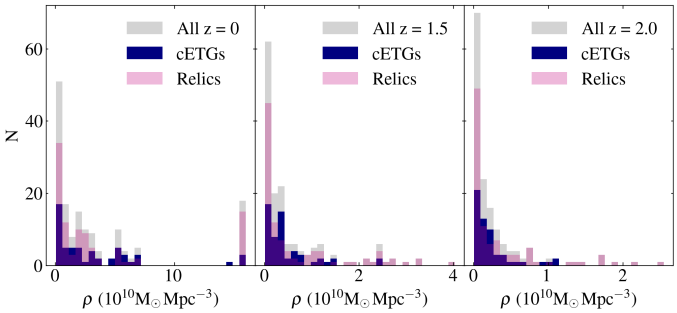

Figure 3. Local density distribution on three different moments, at $z = 0$ (left), $z = 1.5$ (middle), and $z = 2.0$ (right). The Relics and cETGs were traced using the progenitor of the subhalos at each given redshift.

subhalos that experienced significant accretion (50%, 60%, and 70%) overlap with Relic subhalos in each evaluated component. The kinematic behavior of stellar mass distributions, as indicated by the accretion fraction, suggests that the significant accretions in cETGs do not appear to be a key factor in distinguishing them from the Relics pathway sample when assessing overall dynamical perspectives evaluated in each kinematical component computing also, age and metallicities (Fig. 2).

At $z = 0$, the sample's environmental distribution illustrates a wide range of halo masses, equally encompassing Relics, and cETGs. In addition to the overall distribution at $z = 0$, we investigated the evolution of local density (within 2 Mpc) for progenitors at $z = 2$, and $z = 1.5$ (Fig. 3). Our findings indicate a higher number of Relics in denser environments compared to cETGs in the same mass range at all evaluated redshifts. We explore the $F_{disk,\star}$ and $F_{halo,\star}$ dependence on the environment by looking at the subhalos located in a cluster-like halo, to compare with the ones located in the field. This result supports the trends aforementioned, where the similarities among the sample persist even when exploring extreme environmental cases, suggesting that the effects of local galactic dynamics on these objects outweigh the influences from the environment.

Acknowledgements. Conselho Nacional de Desenvolvimento Científico e Tecnológico (CNPq), Coordenação de Aperfeiçoamento de Pessoal de Nível Superior (CAPES), Programa de Pós-Graduação em Física (PPGFis) at UFRGS, Illustris Project & Sociedade Astrônomica Brasileira (SAB).

References

Belli S., Newman A. B., Ellis R. S., 2014, ApJ, 783, 117. doi:10.1088/0004-637X/783/2/117

Buitrago F., Trujillo I., Conselice C. J., Bouwens R. J., Dickinson M., Yan H., 2008, ApJL, 687, L61. doi:10.1086/592836

Flores-Freitas R., Chies-Santos A. L., Furlanetto C., De Rossi M. E., Ferreira L., Zenocratti L. J., Alamo-Martínez K. A., 2022, MNRAS, 512, 245. doi:10.1093/mnras/stac187

Naab T., Johansson P. H., Ostriker J. P., 2009, ApJL, 699, L178. doi:10.1088/0004-637X/699/2/L178

Pillepich A., Springel V., Nelson D., Genel S., Naiman J., Pakmor R., Hernquist L., et al., 2018, MNRAS, 473, 4077. doi:10.1093/mnras/stx2656

Trujillo I., Conselice C. J., Bundy K., Cooper M. C., Eisenhardt P., Ellis R. S., 2007, MNRAS, 382, 109. doi:10.1111/j.1365-2966.2007.12388.x

van Dokkum P. G., Nelson E. J., Franx M., Oesch P., Momcheva I., Brammer G., Förster Schreiber N. M., et al., 2015, ApJ, 813, 23. doi:10.1088/0004-637X/813/1/23

van der Wel A., Franx M., van Dokkum P. G., Skelton R. E., Momcheva I. G., Whitaker K. E., Brammer G. B., et al., 2014, ApJ, 788, 28. doi:10.1088/0004-637X/788/1/28

Zibetti S., Gallazzi A. R., Hirschmann M., Consolandi G., Falcón-Barroso J., van de Ven G., Lyubenova M., 2020, MNRAS, 491, 3562. doi:10.1093/mnras/stz3205

Zhu L., Pillepich A., van de Ven G., Leaman R., Hernquist L., Nelson D., Pakmor R., et al., 2022, A&A, 660, A20. doi:10.1051/0004-6361/20214249